

FMRI GUIDED PERSONALIZATION OF CORTICAL PARCELLATION MAPS AND ITS GRAPH-BASED ASSESMENT IN ALZHEIMER'S DISEASE

Mehmet Said Onay, Umut Küçükaslan

PROBLEM

Cortical parcellations are obtained via structural registration of T1-weighted images of two patients, one of whose parcellation has been previously generated by a medical expert. Although this provides person to person correspondence of anatomical maps, it disregards the functional homogeneity within parcels. The purpose of this project is to improve the 3D human brain cortex parcellation by means of joint structural and functional segmentation and registration. The goal of cortex parcellation is to achieve structurally compact and plausible, functionally homogeneous 3D segmentation of the human brain cortex using multi-modal MRI data. The project involves elastically and iteratively refining an existing cortex parcellation by maximizing the intra-parcel correlation of fMRI BOLD signals. In this project, we also investigate the potential use of personalized parcellation maps in finding biomarkers of Alzheimer's Disease.

METHOD

Assuming functionally homogeneous cortical regions mostly overlap with the structurally obtained counterparts such that the difference between the two arises in the neighborhoods of boundaries of parcels. Around the boundary, we measured a score for each voxel that determines the willingness to be a part of either nearest parcels. A force field is defined according to the scores of voxels to push the boundaries until it reaches an equilibrium. Inverse of this force field is used as a deformation field to warp the 3D image at every iteration. This scheme is repeated until convergence, for which voxels at the boundaries score equally for both of the nearest parcels.

Calculation of the score for a boundary voxel requires defining a correlation cost that accounts for functional connectivity and a volume cost that preserves structural organization of the brain. Correlation cost tries to move the boundary such that the voxel stays at the parcel of its interest after deformation, and is calculated as follows.

For each parcel P_i , time signals x_j corresponding to voxels v_j are stacked into a matrix A_i as columns

$$A_i = [x_1 \quad \dots \quad x_j \quad \dots \quad x_m] \text{ for } v_j \in P_i$$

SVD decomposition of $A_i = U_i \Sigma_i V_i^H$ gives the parcel representative signal r_i as the column of matrix U_i corresponding to the largest singular value in the matrix Σ_i . A voxel at the boundary can either stay whichever parcel it belongs to or merge onto neighboring parcel. Thus, for a specific voxel, only two parcels (current P_c and neighbor P_n) is our concern, and we calculated correlation cost c_j for voxel v_j with time signal x_j as

$$c_j = \frac{x_j^T r_c}{\sqrt{(x_j^T x_j)(r_c^T r_c)}} - \frac{x_j^T r_n}{\sqrt{(x_j^T x_j)(r_n^T r_n)}}$$

c_j can take values in the range $[-2 : 2]$. Higher the c_j value is, the more the boundary is pushed outward and the voxel v_j stays within its current parcel, and vice versa. This movement is either encouraged or suppressed by volume cost, which tries to keep volumes of parcels as close to their initial values as possible, depending on relative volume changes of parcels. Volume cost is calculated as follows.

For each parcel P_i , we calculated percentage of volume changes ΔV_i as

$$\Delta V_i = \frac{V_i^{\text{current}} - V_i^{\text{initial}}}{V_i^{\text{initial}}}$$

In order to compensate volume changes, the boundary should be moved in favor of the parcel whose volume has changed more. Therefore, we paid attention to the difference of volume changes rather than their values. For a boundary voxel v_j with current P_c and neighbor P_n parcels, the difference $\Delta V_n - \Delta V_c$ has range of $(-\infty : +\infty)$. In order to make the range comparable to that of correlation cost, we calculated volume cost a_j for voxel v_j using Sigmoid function as

$$a_j = \frac{1}{1 + e^{-\gamma(\Delta V_n - \Delta V_c)}} - \frac{1}{2}$$

where higher values of a_j tries to move the boundary outward at voxel v_j . Therefore, we have two costs, both of whose positive values implies an outward force at the boundary. Correlation cost tries to cluster voxels with high correlation whereas Volume cost tries to keep the volumes of parcels close to the initial values. We calculated the score s_j for each boundary voxel v_j by combining correlation with a volume constraint as

$$s_j = (1 - \lambda)c_j + \lambda a_j$$

where λ controls the importance given to correlation and volume constraint.

In this algorithm, 3D cortical parcellation image is modeled as an elastic membrane and the deformation field calculated is as follows

Normal vectors are found at each boundary voxel. After scaling with voxel scores found before, they are used as the force at that location. The deformation field is filled with zero vectors except near the boundary. Thus, for a voxel v_j , force field $\vec{F}(v_j)$ is

$$\vec{F}(v_j) = \begin{cases} s_j \vec{n}_j & \text{if } v_j \text{ is boundary voxel} \\ \vec{0} & \text{if } v_j \text{ is not boundary voxel} \end{cases}$$

We smoothed this field with Gaussian kernel to eliminate outliers and updated the parcellation. After iterating this procedure, we obtained the refined cortical parcellation.

Algorithm 1 Cortical Parcellation Refinement

```

1: for i = 1...N do
2:   Find initial parcel volumes  $V_i^{\text{initial}}$ 
3: end for
4: Set  $t = 0$ 
5: repeat
6:    $t \leftarrow t + 1$ 
7:   for i = 1...N do
8:     Find parcel volumes changes  $\Delta V_i = \frac{V_i^{\text{current}} - V_i^{\text{initial}}}{V_i^{\text{initial}}}$ 
9:     Find parcel representative signals  $r_i$  using  $A_i = U_i \Sigma_i V_i^H$ 
10:   end for
11: Find boundary voxels  $B$ 
12: Set  $\vec{F}(v) = \vec{0}$  for  $\forall v$ 
13: for  $v_j \in B$  do
14:   Find unit vector normal to boundary  $\vec{n}_j$ 
15:   Find score  $s_j$  for the voxel as

```

$$s_j = (1 - \lambda) \left(\frac{x_j^T r_c}{\sqrt{(x_j^T x_j)(r_c^T r_c)}} - \frac{x_j^T r_n}{\sqrt{(x_j^T x_j)(r_n^T r_n)}} \right) + \lambda \left(\frac{1}{1 + e^{-\gamma(\Delta V_n - \Delta V_c)}} - 0.5 \right)$$

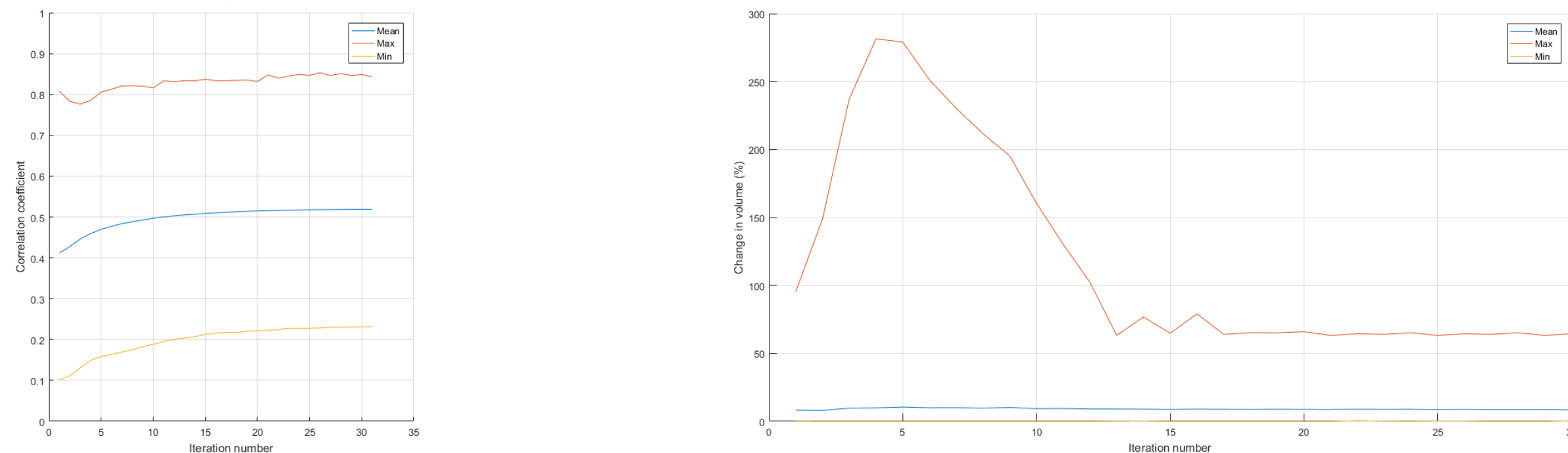
```

16:   Set force  $\vec{F}(v_j) = s_j \vec{n}_j$ 
17: end for
18: Smooth  $\vec{F}(v)$  with Gaussian kernel
19: Warp parcellation map with nearest neighbor interpolator
20: until  $t = M$ 

```

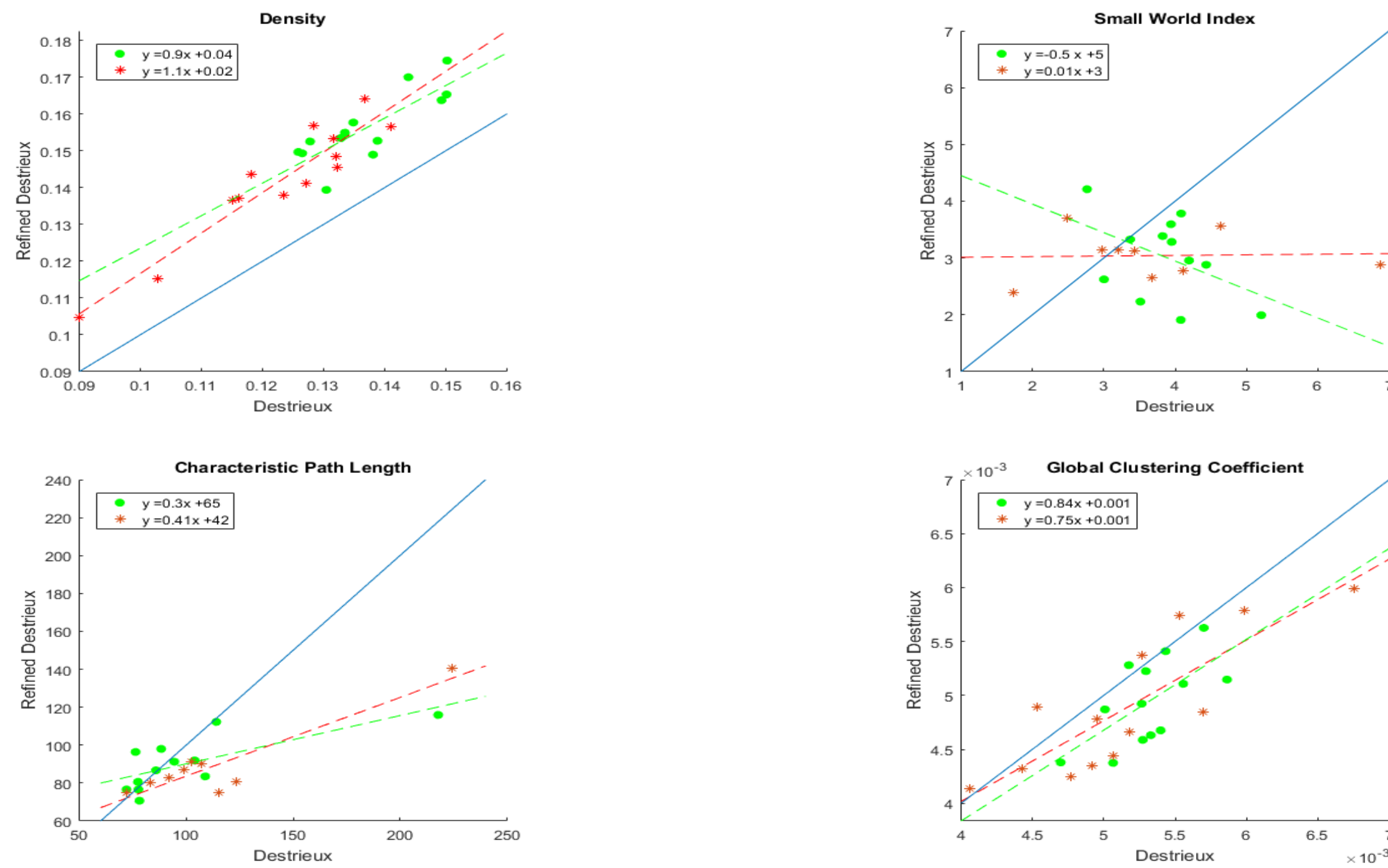
RESULTS

Our novel algorithm is tested on the multi-modal MRI data of 13 healthy subjects and 13 subjects with Alzheimer's Disease(AD). Well-known Destrieux Atlas which divides the brain into 148 parcels is used as the cortical parcellation map. To measure the within-parcel functional homogeneity, Pearson Correlation coefficients of parcels are calculated over iterations.



The first graph above summarizes the change in Pearson coefficients of the cortex parcels through iterations. The mean of the Pearson coefficients of all cortex parcels is increased 20-25% for all subjects. In the second graph, the change in the parcel volumes are shown and the mean of the volume changes of parcels is less than 10% for all subjects. We can also deduce that the volume constraint of the algorithm prevents major changes of parcel structures, since the parcel with the maximum volume change (corresponding to one of the smallest parcels) is confined back after substantial inflation.

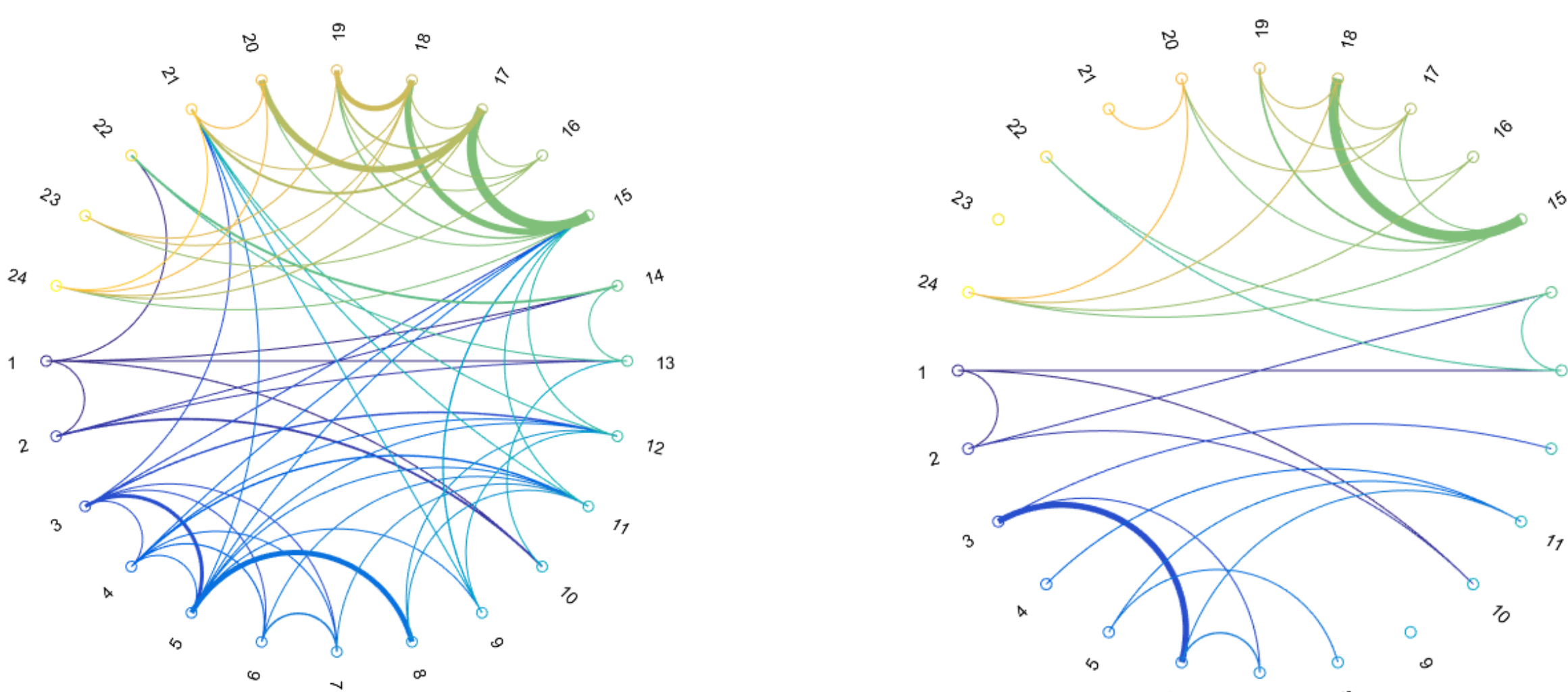
We used the correlation of fMRI BOLD signals as an indicator of functional connectivity in the brain and refined the structural organization accordingly. This notion can be supported with Hebbian theory of synaptic plasticity that is often summarized as "Neurons that fire together wire together". To further our analysis and validate the refining algorithm, we utilized the graph theoretical approach to large-scale structural brain connectivity. The most common technique for studying structural connectivity in the brain is using DWI (Diffusion Weighted Image). We reconstructed the trajectories of axonal fibers by using deterministic tractography and found the structural connectivity weights between parcels. Comparison of the structural networks in healthy subjects and AD patients for both Destrieux Atlas and our refined parcellation is given below.



The graphs above show some of the global network parameters for both of the parcellation maps. Green and red points correspond to healthy subjects and AD patients respectively. The blue line is a reference between parcellations and indicates y=x line. Dashed lines are fitted to the data to ease the comparison.

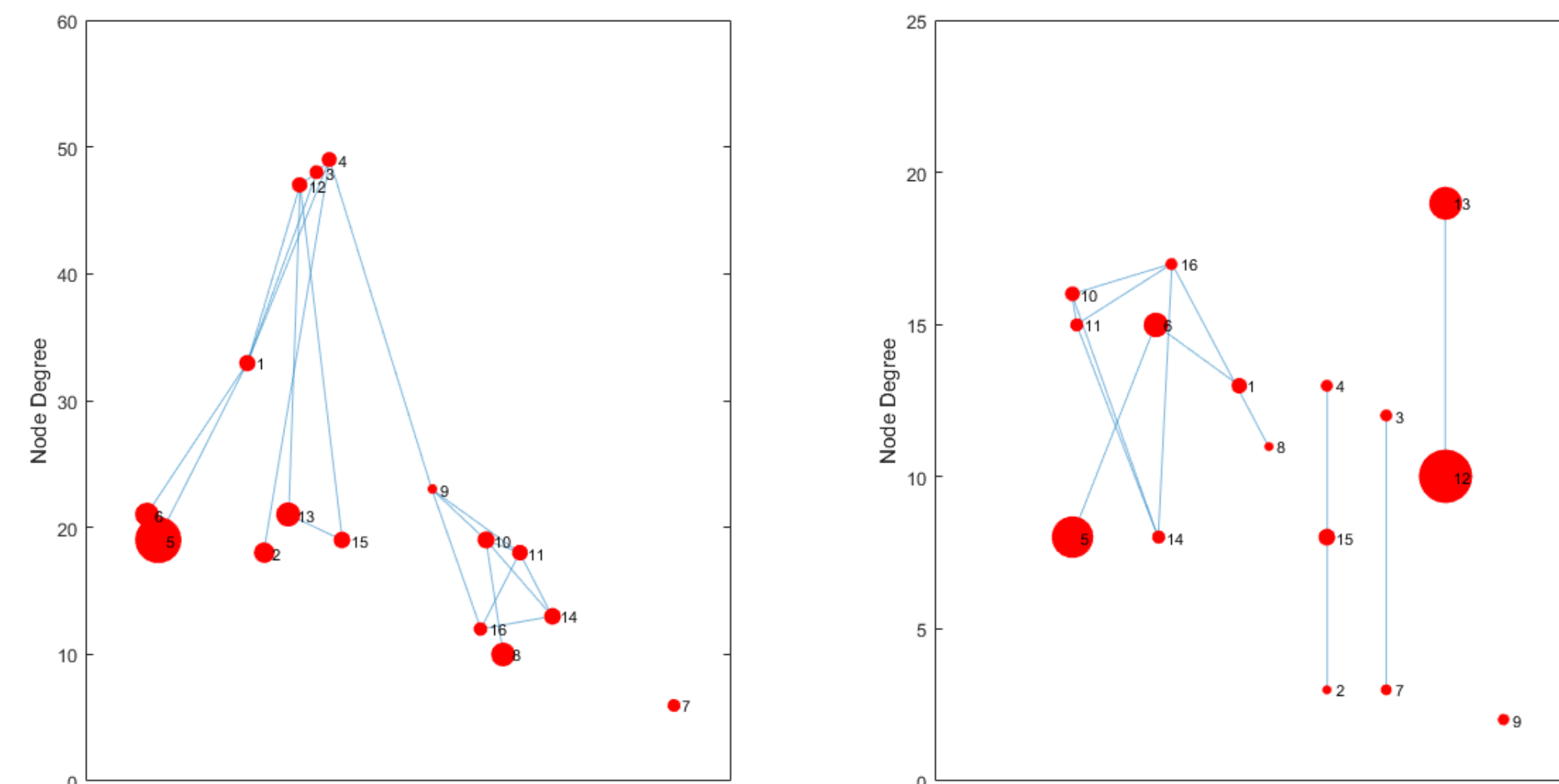
The most obvious result of our refining process was observed in density parameter. Density is the fraction of present connections to possible connections between parcels while connection weights are ignored. The refining algorithm was able to increase density for all subjects, implying a more connected structure. In the small-world index, an inverse relationship is observed between parcellations for healthy subjects. For AD patients, refined parcellation reduced the deviation in small world index. Other global parameters did not yield a definitive difference between parcellations.

It has been appreciated that many neurological and psychiatric disorders (AD included) can be described as disconnectivity syndromes. With this in mind, AD may not affect the large-scale network parameters profoundly and there is still no consensus on how they change in AD. However, it has been established that AD has severe impacts on some sub-networks in the brain: Salience and Default Mode Network(DMN) being the most affected. Salience Network is shown below as a circular graph for healthy and AD subject to illustrate the disconnectivities. Nodes on the perimeter represent the parcels in Salience Network and darker connection colors indicate higher weights.

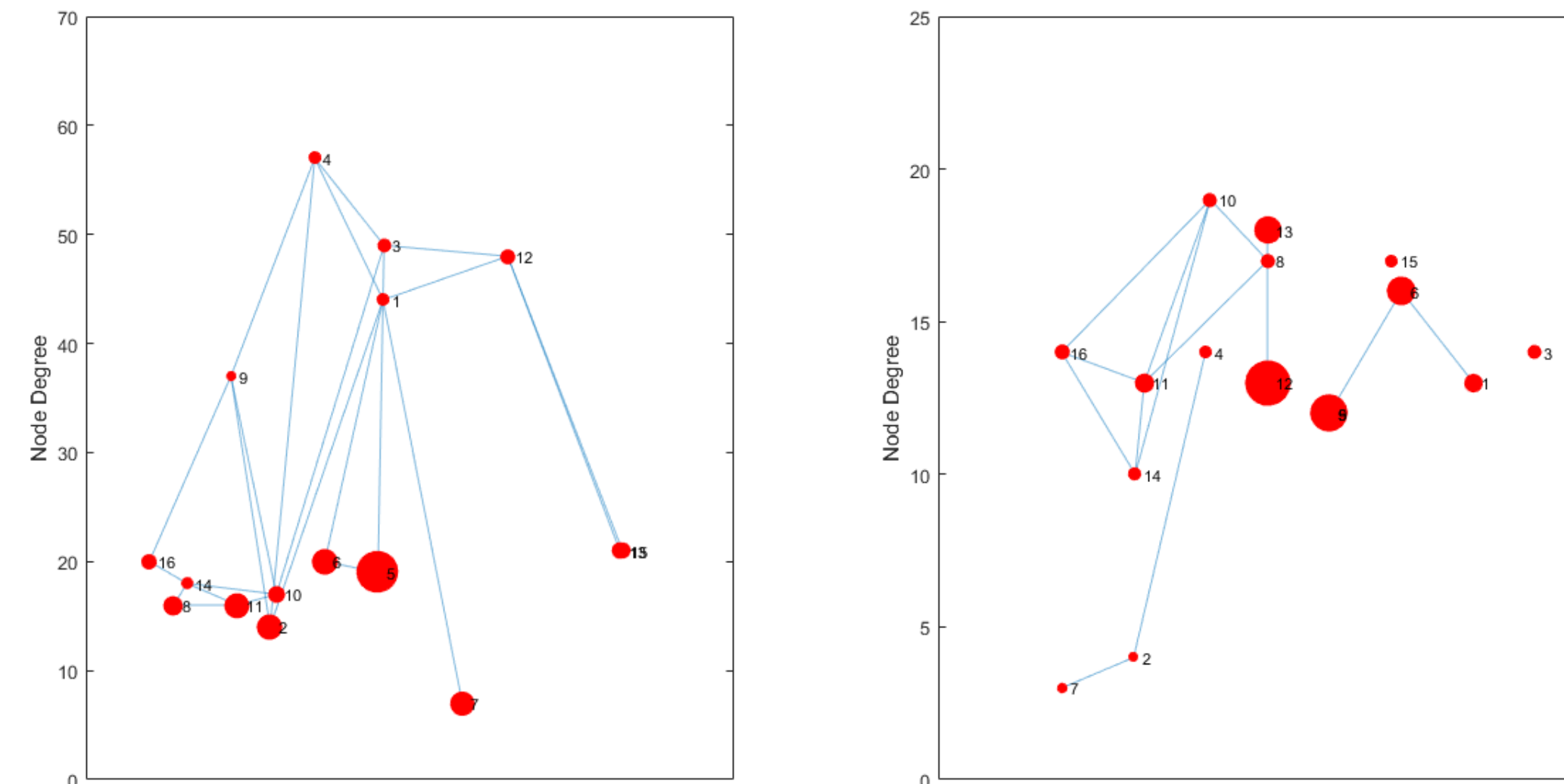


RESULTS

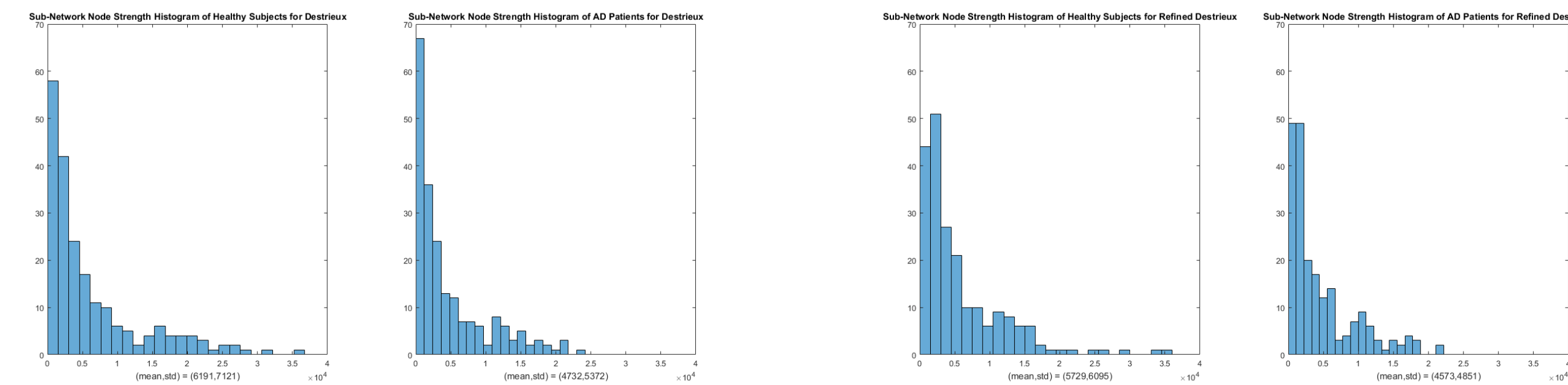
In order to find the distinctions between structural brain networks of healthy and AD subjects, nonparametric Network-Based Statistic(NBS) test is performed for both parcellations and all subjects. Destrieux Atlas identified a sub-network where 9 of the parcels are from DMN and Salience networks with p-value<0.01. Refined parcellation was able to identify 16 parcels from DMN and Salience networks with p-value<0.01. Since this is the most distinct structure between healthy and AD subjects, we continue our comparison of parcellations over this sub-network.



Above graph shows the distinct sub-network organization of a healthy subject (left) and an AD patient (right) with the connectivity matrices calculated from Destrieux. Y-axis denotes node degrees and node size indicates local node clustering coefficients. After refining the parcellation, the sub-network transforms to the image below. Our first finding that the refined parcellation provides a more connected structure still holds for the healthy subject. For AD case, this particular sub-network is severely disconnected. Also in this sub-network, nodes with high clustering coefficients usually have relatively less node degrees in healthy subjects, whereas highly clustered nodes may have relatively higher node degrees in AD.



In this particular sub-network; node degrees, nodal clustering coefficients and node strengths are considered as discrete random variables from two population. Then, Two-sample Kolmogorov-Smirnov test was applied to discriminate healthy subjects from AD patients for both parcellations. Destrieux Atlas was able to distinguish the node degree distributions of healthy and AD subjects with p-value=0.02 and did not give a statistically significant distinction for node strength and nodal clustering coefficient distributions. On the other hand, Refined Destrieux Atlas was able to discriminate all of the three distributions with p-values (0.02,0.01,0.003) respectively.



CONCLUSION

Our refining algorithm gives a personalized brain mapping by increasing intra-parcel correlations of fMRI BOLD signals and preserving person-to-person correspondence of the anatomical structure. Functionally homogenizing the parcellation map makes the large-scale structural network more connected(increasing density) at the expense of decreasing the variation in nodal strength. Utilizing neuronal activation data to have a better estimate of disconnectivity patterns in the brain complements the previous Hebbian concept: "neurons that fire together die together". Personalized parcellation allows more sensitive statistical calculations in the account of graph-based network analysis and can be of use in the pursuit of finding biomarkers of neurodegenerative diseases.

REFERENCES

- [1] Thirion, J. (1998). Image matching as a diffusion process: an analogy with Maxwell's demons. Medical Image Analysis, 2(3), pp.243-260.
- [2] deEtoile, J. and Adeli, H. (2017). Graph Theory and Brain Connectivity in Alzheimer's Disease. The Neuroscientist, 23(6), pp.616-626.
- [3] Tijms, B., Wink, A., de Haan, W., van der Plier, W., Stam, C., Scheltens, P. and Barkhof, F. (2013). Alzheimer's disease: connecting findings from graph theoretical studies of brain networks. Neurobiology of Aging, 34(8), pp.2023-2036.